



Technical Design Paper

AUVSI SUAS 2018

Edhitha Unmanned Aerial Systems, Ramaiah Institute of Technology



Abstract

Edhitha is a team from Ramaiah Institute of Technology, India, which has participated in the SUAS competition since 2011. With the name '*Edhitha*' standing for 'progress in increments', the philosophy adopted by *Edhitha* each year is to incrementally improve its systems and subsequently improve its performance at the SUAS competition. *Edhitha's* approach for the SUAS 2018 was geared towards isolating points of failure from previous mission performances and building a robust and reliable system. After a thorough analysis of the mission objectives, individual subsystems were developed, tested for performance and viability, integrated, and tested for full mission performances. Test results and safety considerations were analyzed during each phase for continual improvement of the system. *Edhitha's* complete mission setup includes a highly improved and capable autonomous navigation module, an ADLC algorithm with multiple failsafe, a stationary and moving obstacle avoidance algorithm, and an air delivery mechanism. All of the previous subsystems rely on a redundant ground communication system and interoperability server. Air delivery and the moving obstacle avoidance algorithm are new additions to the full mission setup. With safety and reliability as the major focus point for this year's competition, *Edhitha* hopes to accomplish all attempted mission objectives and deliver a well-rounded performance at the AUVSI SUAS 2018

Contents

1 Systems Engineering Approach	03
1.1 Mission Requirement Analysis	03
1.2 Design Rationale	04
1.2.1 Airframe Selection Rationale	04
1.2.2 Rationale for Onboard Systems	05
1.3 Programmatic Risks and Mitigation	05
2 System Design	06
2.1 Airframe	06
2.1.1 Structural Tests	06
2.2 Power Systems	07
2.2.1 Servo Load Test	08
2.2.2 Static Thrust Test	08
2.3 Flight Controller	08
2.3.1 Autonomous Flight	08
2.3.2 Ground Control Station	09
2.4 Obstacle Avoidance	10
2.4.1 Stationary Obstacle Avoidance	10
2.4.2 Moving Obstacle Avoidance	10
2.5 Imaging System	10
2.5.1 Geotagging	10
2.6 Object Detection, Classification, and Localization	11
2.6.1 Target Detection	11
2.6.2 Shape Detection	11
2.6.3 Color Detection	11
2.6.4 Optical Character Recognition (OCR)	11
2.6.5 Object Localization, Distortion Modeling, and Orientation	12
2.6.6 Failsafe: Manual Target Detection	12
2.7 Communications and Data Links	12
2.8 Air Delivery	13
2.9 Cyber Security	14
3 Safety Risks, and Mitigations	14
3.1 Operational Safety	14
3.2 Developmental Risks, and Mitigations	14
3.3 Mission Risks, and Mitigations	15
Conclusion	15

1. Systems Engineering Approach

1.1. Mission Requirement Analysis

Edhitha's approach for the 2017-18 academic year was structured towards improving the reliability of the Unmanned Aerial System (UAS) built on the past experiences of SUAS 2017 and 2016, and to refine it to its maximum capabilities. Based on several factors including team experience, risk analysis, and availability of resources, *Edhitha* will attempt the tasks as enumerated in Table 1.

Mission Objective	Specific Mission Objective	Weightage	Status	Requirements
Autonomous Flight	Autonomous Flight	12%	Will accomplish	-Flight Controller (FC) with reliable path planning support -Telemetry modules with an update rate of at least 5 Hz
	Waypoint Capture	3%		
	Waypoint Accuracy	15%		-FC with positioning accuracy to within 20 feet
Obstacle Avoidance	Stationary Obstacle Avoidance	10%	Will accomplish	-Reliable and robust path planning algorithm
	Dynamic Obstacle Avoidance	10%	Will attempt	-Interface real time path planning modification algorithms with FC
Object Detection, Classification, and Localization	Search Area and Off Axis	--	Will not attempt	-Requires camera gimbal -Will not attempt due to unfavorable risk-reward tradeoff
	Characteristics	4%	Will accomplish	-High resolution, low noise, high clarity images
	Geolocation	6%		-Detect image capture and georeference
	Actionable intelligence and interoperability	6%		-Individual interoperability client on each system
	Autonomy	4%		-Low error rate -Robust target characterization workflow
Air Delivery	Delivery Accuracy	10%	Will attempt	-Autonomously operable mechanism -Accurate model to predict the point of impact for the payload
Operational Excellence and Timeline	--	20%	Will accomplish	-Adequate full mission simulations -Well defined team roles and on-field chain of command

Table 1: Mission Requirement Analysis

1.2. Design Rationale

This year’s design rationale was augmented by years of experience at the SUAS, with the 2017 competition as a turning point in terms of learning experience. Several system malfunctions during last year’s mission flight necessitated the development of a more reliable system. The Design Methodology used is shown in Figure 1.

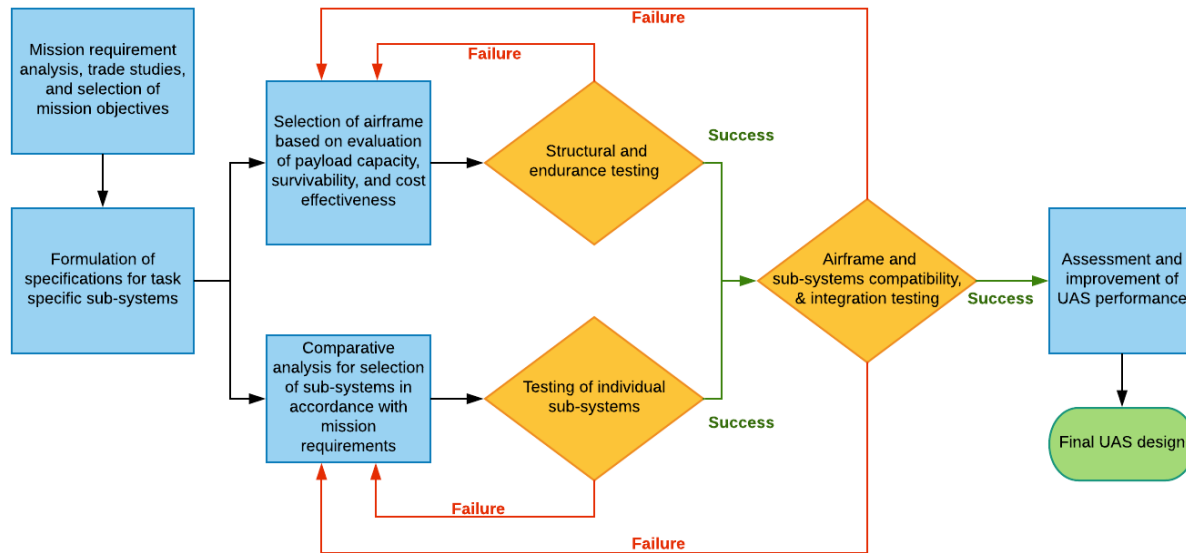


Fig 1: Design Methodology

1.2.1. Airframe Selection Rationale

Given the mission requirements, the factors considered for airframe selection were payload capacity, structural integrity, survivability, and ease of transportation. Off-the-shelf airframes were preferred to shorten the airframe development process as opposed to custom-built airframes. Based on past experiences, foam based airframes were favored due to their reparability and ease of maintenance. A large payload capacity with the ability to integrate a DSLR camera was necessary. Multirotors were not considered due to their inability to provide adequate endurance needed for the mission. Despite their structural simplicity, flying wings are unstable in the pitch and yaw axes, and were disregarded based on previous experience. Fixed wing designs are more efficient for a given payload than multirotors and provide relatively better endurance at higher cruise speeds. Their natural glide characteristics and docile handling offered requisite stability for the mission profile.

Aircraft	Wingspan (in mm)	Maximum take-off weight (in grams)	DSLR Carrying Capability	Take-off method	Configuration
RMRC Anaconda	2060	5500	Yes	Runway required	Fixed wing, inverted V-tail, single pusher motor
Skywalker EVE-2000	2240	4600	Yes	Hand/Catapult launch	Fixed wing, T-tail, twin tractor motors
Believer	1960	4500	Yes	Hand/Catapult launch	Fixed wing, V tail, twin tractor motors
My Twin Dream	1800	5800	No	Hand/Catapult launch	Fixed wing, conventional tail, twin tractor motors

Table 2: Airframe Comparison

After a methodical analysis of the available airframes as shown in Table 2, the team narrowed its options down to the RMRC Anaconda and the Skywalker EVE-2000. These airframes are ideal to house all the required components while providing easy accessibility to the DSLR camera. The team’s previous experience with the Anaconda (SUAS 2015 and 2017) significantly reduced developmental time and improved reliability; and was thus chosen as the airframe for SUAS 2018.

1.2.2. Rationale for Onboard Systems

Multiple components for each subsystem were compared and the chosen product has been highlighted in Table 3.

System	Products considered	Rationale behind the product chosen
Flight Controller	- Pixhawk 2.1 - Pixhawk - Navio2 - Pixhawk Mini	-Open source firmware extensively tested by the UAS community -Substantial reverse compatibility with the Pixhawk, enabling ease of integration with present systems. -Upgraded support and sensors for safety purposes
GPS Module	- HERE GNSS - RTK HERE+ - UBlox M8N	-Inbuilt safety switch and Pixhawk status LED -Cost effective -Supported by the Pixhawk 2.1
Air speed sensor	- MS4525DO -MS5525DO	-Already in use and found to perform reliably
On-board Computer (OBC)	- Odroid C2 - Raspberry Pi-3 - Odroid XU-4 - Intel Edison	-Fast networking benchmark of 1472MiB/s for faster uploads to the server and data transfer to GCS -Uses an eMMC module running the operating system, thus increasing write speeds of images
Imagery	- Nikon D3300 - Sony A6000 - GoPro Hero 6 - MAPIR Survey2 camera	-Higher number of images captured per battery -Higher clarity images than comparable cameras -Compatibility with on board imagery systems
Data Link	- Ubiquiti Bullet M5 - Ubiquiti Nanostation M5 -LiteBeam M5 -airGrid M -Ubiquiti PicoStation M2	-Consistent and robust with its performance throughout previous competitions -Durability, small form factor, and lightweight - Long operational range and reliable data transfer at a rate of 4 MB/s
Geolocation	- Positional data from Pixhawk - Solmeta Geotagger	-Repurposed usage of pose data from existing FC sensors -Solmeta Geotagger is also susceptible to interferences from certain UAS components

Table 3: System Selection Rationale

1.3. Programmatic Risks and Mitigations

Edhitha attempted to foresee factors that could cause delays in development and testing and attempted to mitigate them by ensuring clarity in component availability, scheduling, and team preparedness as tabulated in Table 4.

Risk	Impact	Likelihood	Mitigation
Insufficient unit and integration testing of subsystems	High	Low	-Two well-trained pilots in the team with regularly scheduled flights
Deviation from project timeline	High	Low	-Each task has a specified due date and every delay is closely followed
Component Failure	High	Moderate	-Regular maintenance and post flight monitoring of critical flight systems. -Availability of operational spares is ensured.
Noncompliance with regulations	Moderate	Low	-All required permissions were taken from respective authorities before testing.

Table 4: Programmatic Risks and Mitigation

2. System Design

2.1. Airframe

The RMRC Anaconda has a twin boom inverted V-tail pusher configuration (refer to Fig 2 for dimensions). The fuselage provided sufficient space to place all the onboard components required for the mission. The wings were reinforced using carbon fiber tubes to increase their payload capacity by a factor of 1.4 and minimize wing flexure. The fuselage was similarly reinforced to increase strength to sustain rough landings. Custom mounts were designed to house critical components like the FC and the data modem to secure them during the flight. The aircraft specifications are provided in table 5.

All-up weight	5500 g
Wingspan	2060 mm
Wing Area	4900 cm ²
Length	1410 mm
Endurance	28 minutes
Cruise Speed	18 m/s
Stall Speed	13 m/s

Table 5: Aircraft Specifications

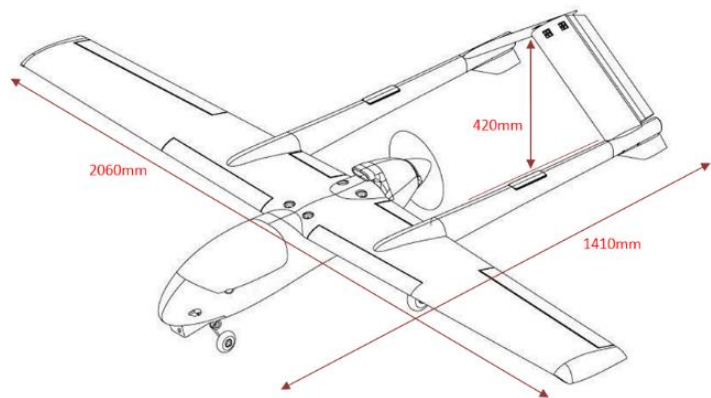


Fig 2: Airframe Diagram with dimensions

2.1.1 Structural Tests

To increase the payload capacity of the airframe and to protect it from damage caused during heavy landings, various retrofits were performed on the airframe. The control surfaces were reinforced with carbon fiber strips and glass fiber to prevent warping. To improve impact and abrasion resistance, the leading edge and tips of the wings were covered with adhesive backed fiberglass. The wings of the Anaconda in stock configuration have two Carbon Fiber tubes functioning as alignment and structural spars in the wings. In order to ensure the payload does not cause any variability in flight characteristics due to wing flex, the wings were structurally reinforced with additional carbon fiber tubes. Wing loading tests were performed with simulated loads on its wingspan in order to assess the

effectiveness of the reinforcements. Significant reduction in wing flex was observed with the reinforcements as shown in Fig 3.2 when compared with Fig 3.1.

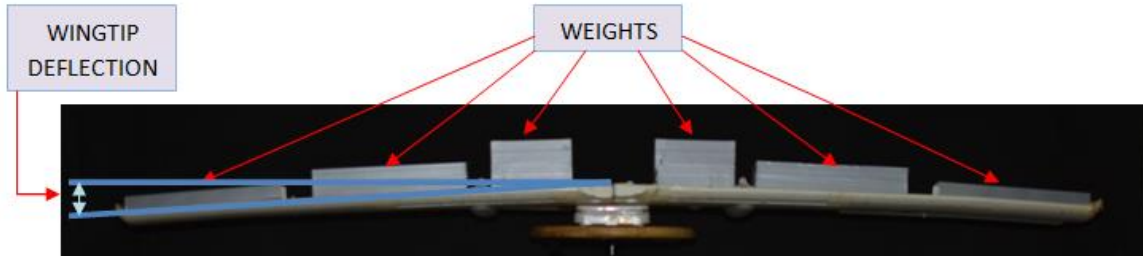


Figure 3.1: Wing Flex before reinforcement

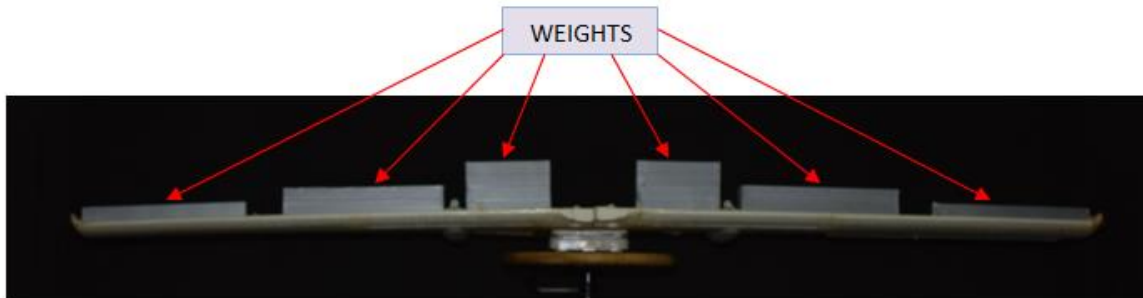
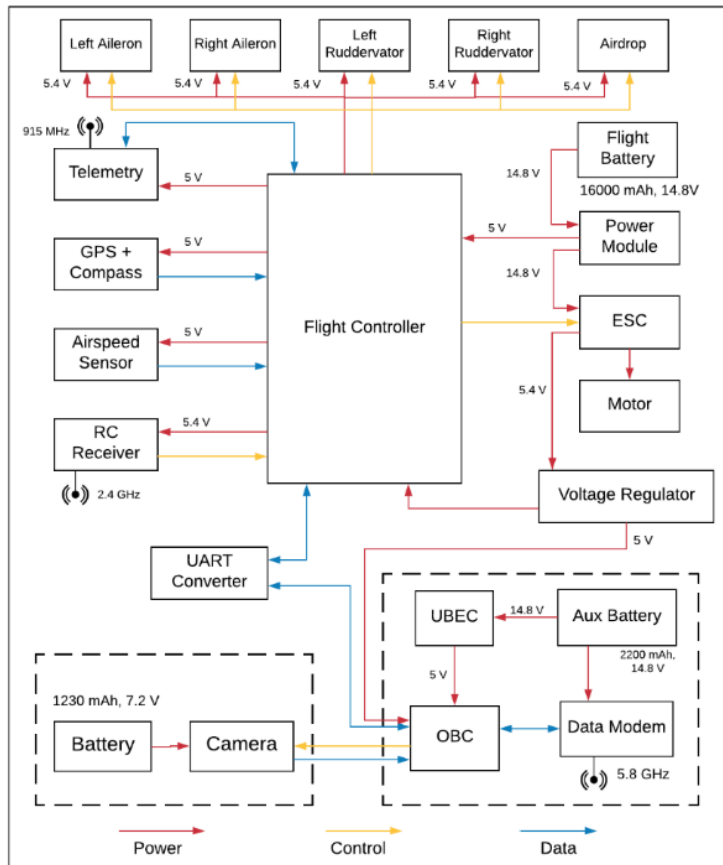


Figure 3.2: Wing flex after reinforcement

2.2. Power Systems



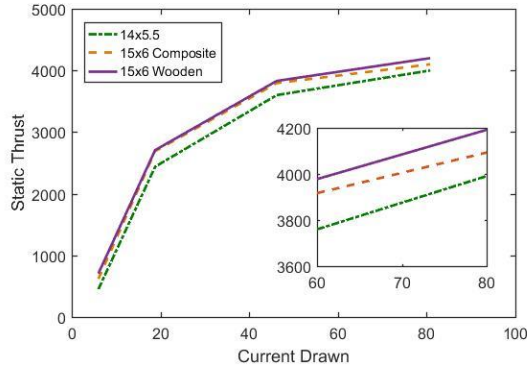
To isolate power system failure, each system in the UAS has a dedicated power supply. The T-motor AT3520 1300W 880K_v motor, used for propulsion is powered using a 4S 16000 mAh Lithium Polymer battery. The motor draws a peak current of 90 A, and is therefore connected via a Castle Phoenix Edge 100 A Electronic Speed Controller. A dedicated 4S 2200 mAh Lithium Ion battery is used to power the OBC and the data modem through a Battery Eliminator Circuit. The camera is powered by a 1230mAh 7.2V Lithium Ion battery which is capable of taking up to 700 pictures on a full charge. The UAS clocked an average flight time of 28 minutes during the full mission test flights. Refer to Fig 4 for a detailed layout of the power system.

Fig 4: UAS Layout and Power Systems

2.2.1. Servo Load Test

In order to verify servo reliability, the servos were subjected to multiple stress tests. A standardized servo horn was used with incremental weights kept at a known distance to identify the maximum torque. At 4.8V, the servos produced 4.39 kg-cm of torque at a speed of 0.15 sec/60° at the ailerons and 3.6 kg-cm at a speed of 0.13 sec/60° at the ruddervators.

2.2.2. Static Thrust Test



The aircraft is propelled by a 1300 W, 880 Kv brushless DC motor coupled with a 100 A ESC. The team’s decision of attempting airdrop was a deciding factor while choosing a propeller because of higher thrust requirement. Thrust tests were performed on a thrust rig for the selected propellers, and were tested at pre-set values of throttle percentage. A graph of Current drawn vs Static thrust generated is shown in Fig 5. The 15x6 wooden propeller provided 4200 gm of thrust with a peak current draw of 90A.

Fig 5. Current drawn vs Static thrust generated

2.3. Flight Controller

The Pixhawk 2.1 was the chosen FC for this year. The FC was an improvement over the previously used Pixhawk due to enhanced flight performance attributed to a robust sensor suite, while also being compatible with the existing equipment. In addition to 8 standard PWM outputs, the FC provides 6 auxiliary PWM outputs, one of which is used to actuate the air delivery mechanism. It has an EMI filtered telemetry port which is powered directly from the power brick to improve link stability. The FC supports dual GPS sensors to enable improved navigation accuracy and reliability in the event of failure of a single GPS unit. An image of the FC is provided below in Fig 6

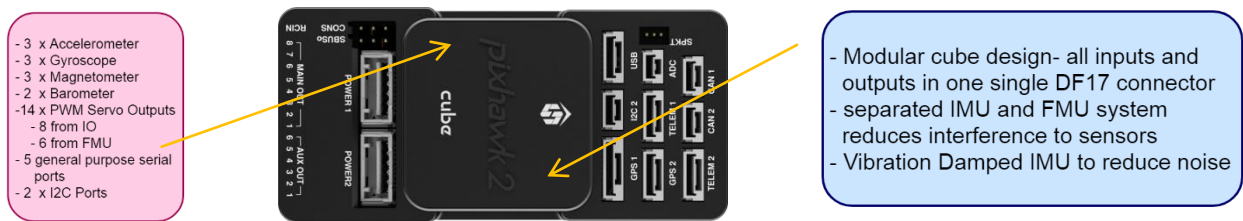


Fig 6: Pixhawk 2.1

Arduplane 3.8 was chosen as the firmware for the FC due to its proven capability and extensive community support. The Firmware uses Extended Kalman Filters for state estimation of the UAS and filters out erroneous sensor readings in the event of sensor failure. Further, the firmware has an inbuilt capability of autotuning the FC.

2.3.1. Autonomous Flight

To achieve autonomous flight, the PID (Proportional Integral Derivative) controllers were tuned to provide accurate roll and pitch responses as shown in Fig. 7. The graph shows favorable response from the UAS to demanded inputs and signifies a well-tuned control system. The pitch and roll follow commanded values closely with minimal lag.

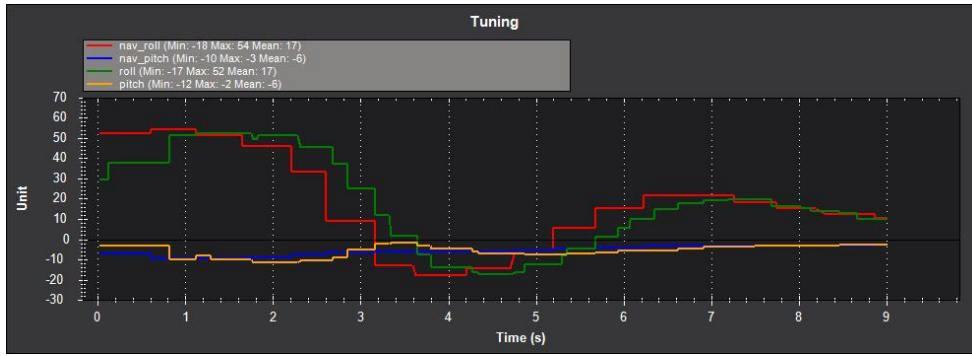


Fig 7. Tuning Response

*nav_roll = demanded roll
roll = achieved roll*

*nav_pitch = demanded pitch
pitch = achieved pitch*



Fig 8.1: Before tuning L1



Fig 8.2: After tuning L1

The PID control loop was tuned to allow for adequate performance in the pitch and roll axes, the L1 controller was tuned for waypoint transitions to enable adherence to the desired flight path. Figures 8.1 and 8.2 show the path tracking before and after tuning the L1 controller.

The flight-plan was designed to perform the air delivery task autonomously. To increase the endurance, team plans to attempt the air delivery task immediately after waypoint navigation. This mission strategy reduces the effective payload weight while attempting other tasks. The competition rules necessitate Return to Launch (RTL) and flight termination, which were accomplished by setting the appropriate failsafe during mission planning.

2.3.2. Ground Control Station

Mission Planner, an open source software was chosen to be the Ground Control Station (GCS). The HUD is accompanied by a map with an overlay which shows the position of the aircraft and the flight-plan, including mission progress as seen in Fig 9. The GCS is used to prepare flight plans to accomplish autonomous navigation and air delivery. It is also used to configure and tune the FC, and monitor UAS behavior during the mission.

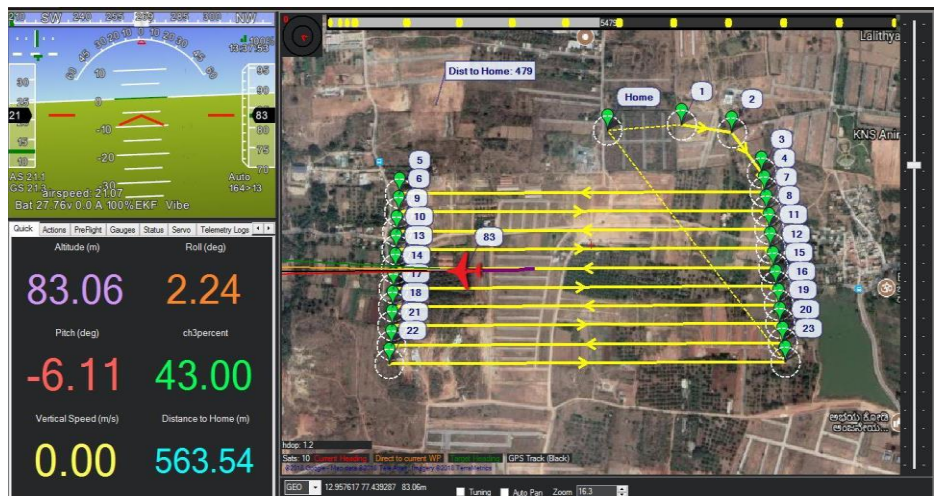


Fig 9: Ground Control Station

2.4. Obstacle Avoidance

2.4.1. Stationary Obstacle Avoidance

The stationary obstacle avoidance algorithm selects an optimum path from all possible flight paths which are generated by an iterative process between two waypoints while accounting for obstacles provided by the interoperability system.

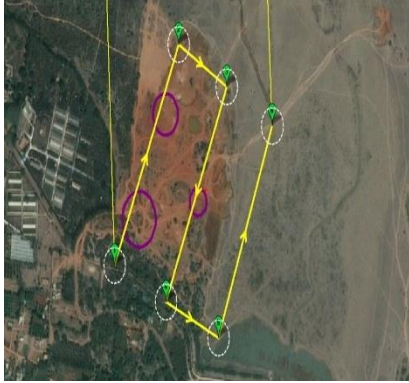


Fig 10.1: Original Path

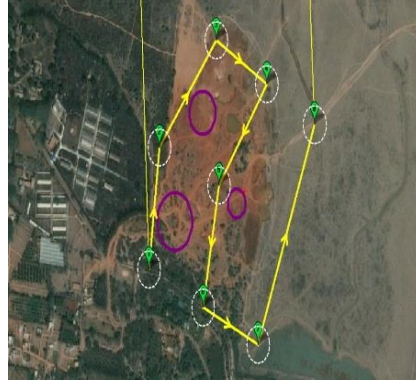


Fig 10.2: Modified Path

The algorithm is modeled as an optimization problem minimizing the distance to the destination. The process involves simulating the UAS as a flock of birds where in each iteration the movement of an individual candidate is influenced by its own local position and the best known position found by other candidates. These best known positions are then sampled at equal intervals to derive new waypoints, and are then uploaded to the FC as a modified flight plan as shown in figures 10.1 and 10.2.

2.4.2. Moving Obstacle Avoidance

A real time obstacle detection algorithm was designed to check for obstacles (both stationary and moving) within a sphere of suitable radius R with the UAS as its centre - called the Sphere of Influence (SoI). The flight plan does not change until an obstacle is detected within the SoI. Once an obstacle is detected, a query is initiated to generate a new path within C_{free} (C_{free} is the Configuration Space devoid of all obstacles) to the next waypoint, which is updated using telemetry. A Rapidly-exploring Random Tree (RRT) algorithm was used to search the spaces and generate new paths whenever a query is initiated. There were modifications made to the RRT algorithm to satisfy kinematic and dynamic constraints (velocity and acceleration bounds) of the UAS while generating new paths. This approach ensured minimal changes to the existing flight plan.

2.5. Imaging System

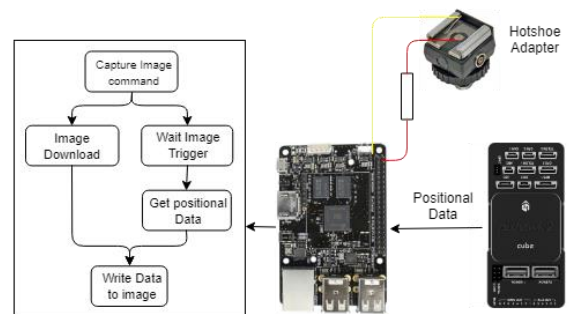
The Nikon D3300 camera equipped with a 35mm wide angle prime lens was used. The camera is capable of capturing 24MP images at the rate of 1 image per second. The images obtained at 120 m altitude had a ground footprint of 52 m length and 85 m width in landscape mode. Considering the UAS ground speed of 18m/s and the image capture rate of 1 image per second, an average overlap of 50% was achieved which ensured multiple occurrences of the target.

The OBC was used to interface the camera with the GCS. An open source Application Program Interface (API) called 'gphoto2' running on the OBC was used for image capture and transfer.

2.5.1 Geotagging

Geotagging is handled by the OBC using pose data from the FC. The OBC uses two synchronous process threads to download an image from the camera while simultaneously watching for trigger action to attach pose data to that image (Refer to Fig 11). The trigger action is detected as a falling edge signal using the hot-shoe adapter to ensure that there is no latency between the camera trigger and acquisition of data.

Fig 11: Geotagging Mechanism



2.6. Object Detection, Classification, and Localization

The process for automatic object detection, classification and localization has been described below.

2.6.1. Target Detection

Images acquired by the Nikon D3300 are relayed to the GCS via the on board communication system. The obtained images are first converted to the Hue Saturation Value (HSV) color space, and a saliency map that highlights the potential targets by subtracting the average HSV channels for the entire image from each individual pixel is generated. The Maximally Stable Extremal Region algorithm (MSER) is employed to detect and highlight boundaries of potential targets. These boundaries are used for masking the region of interest, which are cropped for further processing.

2.6.2. Shape Detection

The cropped images are subjected to iterative erosion and dilation to highlight their boundaries. An image classifier built upon Tensorflow was trained on shape templates derived from the dimensions as stated in the rule book. A confidence value is generated from the classifier indicating the accuracy of detection.

2.6.3. Color Detection

The target crops are converted to the HSV color space and subjected to a K-means clustering algorithm to partition the image into 3 different clusters. The cluster associated to the background is eliminated, and the remaining two clusters (corresponding to shape and letter) are identified by their size - the smaller cluster corresponds to the alphanumeric character and the larger cluster corresponds to the shape. The colors of these clusters are classified accordingly by comparing the HSV values to a predefined range. Fig 12 depicts the color detection workflow

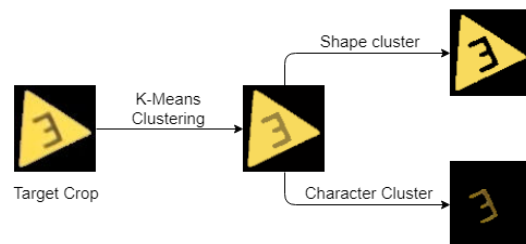


Fig 12: Color Detection Workflow

2.6.4. Optical Character Recognition (OCR)

Character recognition is carried out using an open source engine called Tesseract. Since Tesseract is independent of orientation and calculates a robust confidence level, it is employed to detect the alphanumeric character with a threshold confidence set to 80%. To improve the accuracy and confidence of recognition, the alphabet clusters are subjected to secondary processing to obtain a skeletal character outline as shown in figure 13.

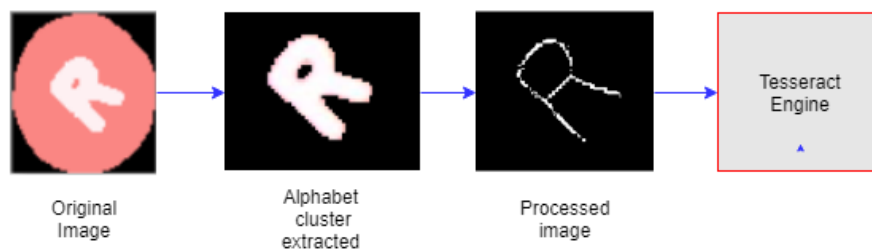


Fig 13: OCR Diagram

2.6.5. Object Localization, Distortion Modelling, and Orientation

Object localization is dependent on the accurate representation of the image via the optical path of the lens. Distortion modelling of the camera lens was performed to account for irregularities commonly observed in off the shelf cameras. The distortion coefficients for the camera+lens setup were obtained by using OpenCV and were used to correct the images accordingly which yielded more accurate results in localization of the objects.

The targets were localized by calculating the distance between the center of the image and the centre pixel of the target. This distance along with the coordinates and orientation of the image was then used to calculate the latitude, longitude and orientation of the target conforming to WGS84 standard with the help of GeoGraphicLib libraries.

2.6.6. Failsafe: Manual Target Detection

A Manual User Interface (UI) was developed as a redundant measure to manually detect, characterize and localize the targets. The detected targets can be sent to Interoperability server from the Manual UI as shown in figure 14.



Fig 14: Manual UI Workflow

2.7. Communications and Data Links

The communication system is decomposed into three independent data links as shown in Fig 15.1 and 15.2

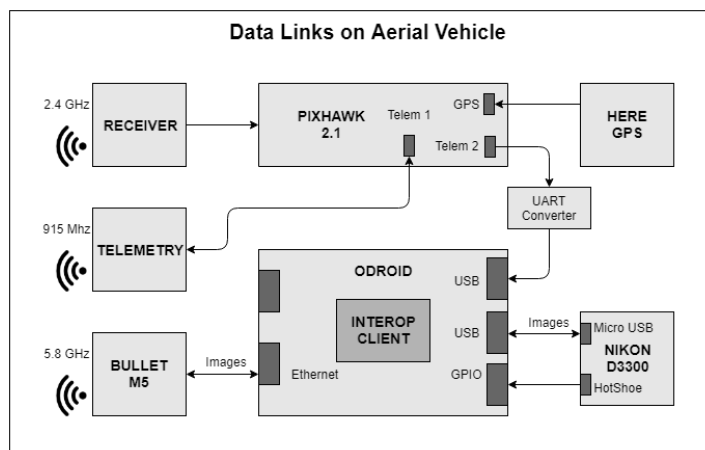


Fig 15.1: Data Links on the UAV

I. 915 MHz Data Link - Telemetry and Autonomous Navigation : The 915MHz link uses the MAVLink (Micro Air Vehicle Link) protocol to establish a telemetry link for the FC and GCS. RFD900x modules, operating at 1000mW are used to ensure high signal strength and data transfer rates of 5Hz.

II. 5.8GHz Data Link - Imagery and Secondary Telemetry : This data link is used to communicate with the OBC and uses the Ubiquiti NanoStation M5 and the Ubiquiti Bullet M5. Primarily used for image transfer, it also serves secondary data link for the FC in the event of failure of the 915 MHz link.

III. 2.4GHz Data Link - Manual Flight Control : The 2.4GHz link serves as the radio control link for the safety pilot.

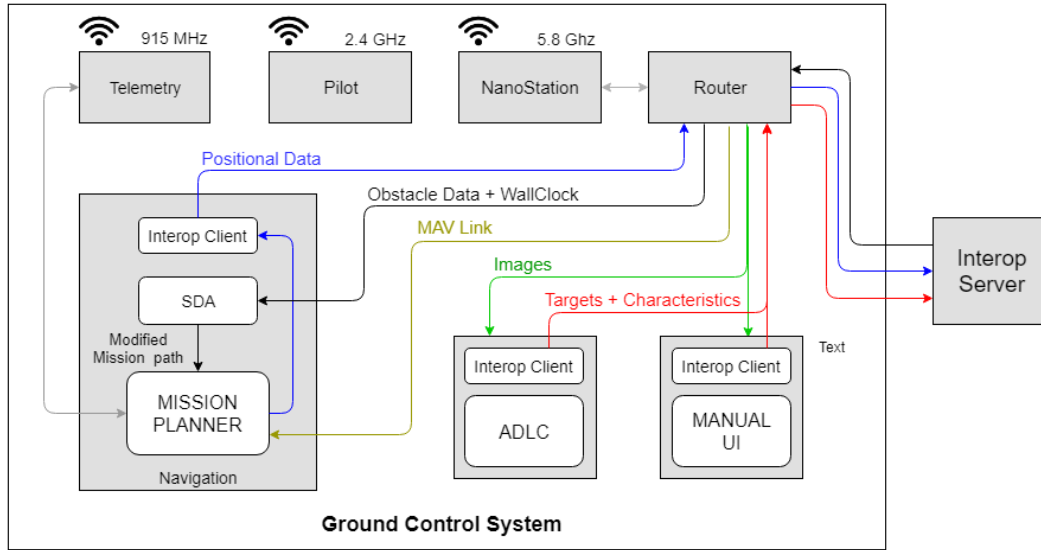


Fig 15.2: Data Links on the GCS

2.8. Air Delivery



Fig 16.1: Airdrop Mechanism with bottle (Side view)

The bottle delivery mechanism (Refer to Fig16.1 and 16.2) was designed to be robust and lightweight. The optimized design weighs 35 grams and was tested with a payload of weight 500g, verifying a designed safety factor of 2:1. When triggered, the kinematic linkage is actuated, allowing the bottle to fall due to its own weight. The assembly is bolted to the belly of the plane and kept at the center of gravity to ensure continued stability of the UAS after the payload drop. The release mechanism is remotely triggered by the FC based on specified drop coordinates, along with a built in redundancy for a manual release in the event of an unforeseen FC error.

The trajectory of the bottle is modeled by the following equation:

$$S = \sqrt{\frac{2H}{g}} \left(\frac{\partial x_{pr}}{\partial t} \right) + \frac{H}{g} \left(\frac{\partial^2 x_{pr}}{\partial t^2} \right)$$

Where,

S	=	Distance covered by the payload in x-direction
$\frac{\partial x_{pr}}{\partial t}$	=	Instantaneous velocity in x- direction
$\frac{\partial^2 x_{pr}}{\partial t^2}$	=	Instantaneous acceleration in x-direction
H	=	Height of the UAS at the time of payload drop
g	=	Acceleration due to gravity

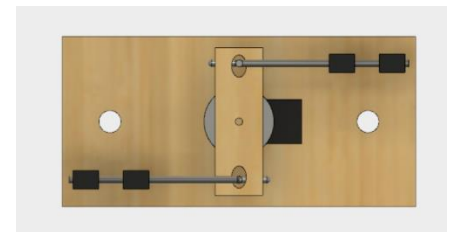


Fig 16.2: Airdrop Mechanism (Top view)

Note: Errors were further minimized using the data obtained from the practice flights.

2.9. Cyber Security

Modules involved in data transfer and data processing have added measures to improve security and reliability. These measures involve modifications in configuration settings, as well as the usage of certain features and software packages. They are as follows:

1. The OBC has been configured to control both the imagery and the navigational subsystem in the event of complete loss of link between the UAS and GCS.
2. Communication between the OBC and the GCS is achieved via SSH (Secure Shell) that makes use of cryptographic network protocols to ensure a secure channel for communication
3. Rsync, a file synchronization command in Linux is used to transfer images between the UAS and GCS. This command was configured with a list of “host systems” which can solely run rsync.
4. The router chosen by *Edhitha* is equipped with MAC-filtering, a utility which only allows authorized computers to access the GCS network and blocks unknown devices.
5. FHSS (Frequency Hopping Spread Spectrum) is made use of due to its high resistance towards narrow band interference, and its reliability in ensuring a secure connection. This is done by rapidly switching a carrier among multiple frequencies.

3. Safety, Risks, and Mitigations

Safety was the top priority for the team this year, and various measures were taken to mitigate all the possible risks during the development of the UAS.

3.1. Operational Safety

- A safety checklist is utilized at preflight and post flight stages.
- Temperatures of critical components such as ESC, motor and battery are measured before and after the flight to monitor component health.
- Batteries are checked for surface cuts, structural damage and insulation quality of the power cables before and after flights.
- Vent holes were added to the fuselage to enable forced convection, thus ensuring heat dissipation from heating components.
- A procedural arming check is conducted prior to flight. A physical connection, an arm switch, and a signal from the navigational system is needed before supplying power to the motor. This prevents propeller inflicted injuries on the field.

3.2. Developmental Risks and Mitigations

Expected developmental risks were enumerated along with their impact and likelihood. A mitigation procedure was then developed for each scenario in the reverse order of their impact. The developmental risks and their mitigation strategies are tabulated in Table 6.

Risk	Impact	Likelihood	Mitigation Strategy
Loss of airframes and subsystems during test flights	High	Moderate	-Back up systems are constantly kept ready in flight ready condition.
Damage to airframe and subsystems during development.	Moderate	Moderate	-Each step of development is planned considering all risks before implementation. -The team is trained sufficiently to ensure that all components are dealt with care.

Errors leading to injury during fabrication and modification	Moderate	Low	-A safety checklist is followed thoroughly by every team member. -Each team member is trained in safety protocols.
--	----------	-----	---

Table 6: Developmental Risks and Mitigation

3.3. Mission Risks and Mitigations

The safety risks posed by the competition mission, autonomous flight, and testing and their mitigation are explained in Table 7

Risk	Impact	Likelihood	Mitigation Strategy
Loss of RC link to the UAS	High	Moderate	-Preflight range tests and FC failsafe such as RTL
Loss of acquired data	High	Low	-All data acquired is backed up to camera and OBC.
Unauthorized air delivery	High	Low	-Air delivery mechanism is triggered by FC only when pre-set location is reached.
Servo failure or incorrect wiring	High	Low	-Frequent maintenance of all flight systems. -Checklists for both pre and post flights are maintained and followed to constantly monitor UAS health.
Temporary Loss of telemetry link >30 seconds	High	Low	-RTL is triggered by the FC.
Loss of Telemetry link >3 minutes	High	Low	-Controlled flight termination as per mission requirements

Table 7: Mission Risks and Mitigation

Conclusion

The development of the UAS for the SUAS 2018 provided unique challenges for the team. Each subsystem had been rigorously tested at the SUAS 2017 and 2016, and were honed to their greatest capabilities. Committed to safety and reliability, the team emphasized on implementing several redundancies and worked on addressing every possible point of failure. Multiple retrofits were identified that allowed the team to execute the mission tasks more efficiently, while simplifying the overall system integration. With several test flights and a proven accuracy in achieving the objective requirements, team *Edhitha* is confident in its UAS' ability of displaying an impressive performance at the SUAS 2018.

List of Team Members

Aditya S Patil	: Software subteam
Adithya Narayan Badanidiyoor	: Software subteam
Anmol Kathail	: Mechanical subteam
Aryaman Bansal	: Mechanical subteam
Lohith N V	: Navigation subteam
Miskin Dash	: Mechanical subteam
Mohammed Naveed Shaikh	: Mechanical subteam
Murali Manohar S Kumar	: Software subteam
M. P. Venkatesh Bharadwaj	: Team Lead, Navigation subteam
Reuben O Jacob	: Mechanical subteam
Roopak Srinivasan	: Software subteam
Suhas Nagaraj	: Mechanical Subteam
Sushanth Jayanth	: Safety pilot, Mechanical subteam
Vageesha Pathak	: Navigation subteam
Vivek Kumar Singh	: Navigation subteam

Faculty Advisor

:Gururaj Bhardwaj
:Dr. S. Sethu Selvi

Team Mentors

: Ankan Dutta
: Arjun Jagdish Ram
: Cholpady Vikram Kamath
: Deborshi Goswami
: Gandhar Ajit Kunte
: Gaurav Chhikara
: Praneeta Mallela
: Sriraghav Sridharan
: Vishnu Byatarayanapura Nagendra
: Vishwanathan Ramanathan